# Distribution and Characterizations of Liquefaction of Celluloses in Sub- and Super-Critical Ethanol

Chao-Yang Zheng, Hong-Xiu Tao, and Xin-An Xie *

Effects of reaction conditions (temperature, retention time, and cellulose/ethanol ratio) on biomass liquefaction in sub- and super-critical ethanol were investigated in this work. The liquefaction system was divided into the following fractions: a volatile organic compounds fraction, a gas fraction, a heavy oil fraction, a water-soluble oil fraction, and a solid residue fraction. Results showed that for three samples, the SR yield of microcrystalline cellulose was highest compared with corn stalk cellulose and rice straw cellulose at the same temperature, while the HO yield was lowest in the liquefaction process. At the same retention time in super-critical ethanol, the SR yield of microcrystalline cellulose was highest, suggesting that the microcrystalline cellulose was difficult to liquefy. The effect of different samples on liquefaction in ethanol with various cellulose/ethanol ratios can be clearly seen from the distribution yields. The FT-IR analysis of the solid residues showed that the structure of celluloses changed after liquefaction. The GC-MS analysis showed that the volatile organic compounds, water-soluble oil, and heavy oil comprised a mixture of organic compounds, which mainly included furfural, acids, furans, esters, and their derivatives. XRD analysis revealed that the decomposing reaction primarily occurred within amorphous zones of the celluloses at the low temperatures.

*Keywords: Liquefaction; Cellulose; FT-IR; XRD; GC-MS*

*Contact information: College of Food Science, South China Agriculture University, Guangzhou 510640, China; * Corresponding author: xinanxie@scau.edu.cn*

## INTRODUCTON

The demand for energy has been increasing dramatically due to the rapid increase in the world's population and developing technologies. Meanwhile the current energy resources have limited reserves and are decreasing (Ozcimen and Karaosmanoglu 2004). Today, biomass is considered a renewable resource with high potential for energy production. Biomass can be converted to various forms of energy through numerous thermo-chemical conversion processes, depending upon the type of energy desired (Yanik *et al.* 2007).

Among the many thermo-chemical procedures, biomass liquefaction into liquid fuel is a promising one, during which the common products are gas, liquid, and char. Liquefaction has many advantages such as, (1) The presence of solvent dilutes the concentration of the products, thus tending to minimize cross-linked reactions and reverse reactions, and (2) The processing temperature is relatively low (less energy consumption) in comparison with other thermo-chemical processes (such as pyrolysis and gasification) (Liu and Zhang 2008). Some articles have reported on the liquefaction of biomass; the presence of solvents has been shown to effectively lower the viscosity of heavy oil derived from biomass liquefaction (Demirbas 2000).

The degradation of biomass cannot be described by detailed chemical reaction pathways with well-defined single reaction steps. The reason is that biomass is a combination of cellulose, hemicelluloses, and lignin, and these components interact with each other, leading to very complex chemistry (Kruse and Gawlik 2003). The knowledge about thermal characteristics and decomposition mechanism of biomass is considerably important for optimization of the conversion process and efficient utilization of the liquid products (Liu *et al.* 2011a,b). Thermogravimetric analysis (TGA) is one of the most common techniques used to rapidly investigate and compare thermal events and kinetics during the combustion and pyrolysis of solid raw materials (Gil *et al.* 2010). Recently, many researchers have evaluated these characteristics including kinetic parameters on different biomasses and different dynamic conditions under inert atmospheres by TGA (Simkovic and Csomorova 2006; Munir *et al.* 2009; Van de Velden *et al.* 2010). The liquefaction process in solvents shows similarities but also significant differences compared with TGA. The solvents can react with biomass, and they also serve as the reaction medium. Therefore, the TGA cannot be used to investigate the thermal characteristics and mechanism of biomass liquefaction in the presence of solvents. In the previous work, the lump analysis of biomass liquefaction in ethanol was studied based on the characteristics of material and products, and lump analysis was found to be effective for study of biomass liquefaction (Liu *et al.* 2011c, 2012a,b). Therefore, analysis of the complex reactions, which occur in the liquefaction of biomass, is important to the description of the reaction behavior and to the optimization of the operating conditions. Cellulose is the structural basis of plant cells and the most important and abundant natural substance. Cellulose molecules are bound to each other by inter- and intra-molecular hydrogen linkages through their hydroxyl groups. Therefore, cellulose molecules form crystal structures under normal conditions, and crystalline cellulose is difficult to decompose. Direct liquefaction of biomass in sub- and super-critical solvent (*e.g.*, water, alcohols, and phenol) has proven to be an effective approach to convert lignocellulose materials into low molecular weight chemicals (Wang *et al.* 2009).

To the best of our knowledge, there are few reports on analysis of cellulose liquefaction in sub- and super-critical ethanol. In the present study, three different celluloses (cornstalk cellulose, rice straw cellulose, and microcrystalline cellulose) were liquefied in a 1 L batch reactor at a temperature range of 200 to 330 °C, a holding time of 0 to 130 min, and different cellulose/ethanol ratios (1/30, 1/15, 1/10, and 1/6). The effects of reaction conditions on the yields were investigated, and the main characterizations of liquefaction products were analyzed by GC-MS, X-ray diffraction and FT-IR spectroscopy.

## METHODS

### Materials

Cornstalk and rice straw were obtained from Guangdong province in China. The samples were milled and sieved through a 40-mesh screen, then dried at 105°C for 24 h. The dried biomass powder (cornstalk and rice straw) was first extracted with chloroform-ethanol (2:1, v/v) in a Soxhlet extractor for 6 h so as to remove the extractable materials, and the meal was allowed to dry in an oven at 90°C for 24 h. The dewaxed powder (15 g) was delignified with 6% sodium chlorite at pH 3.8 to 4.0 and adjusted with acetic acid at 75°C for 2 h (Lawther *et al.* 1995). The residue was subsequently washed with distilled

water and ethanol and then oven dried at 90°C for 24 h. The holocellulose obtained was then soaked in 250 mL of distilled water. The mixture was successively extracted at 23°C with 7.5% NaOH for 2 h and 17.5% NaOH for 2 h. The insoluble residue (cellulose) was collected by filtration, washed thoroughly with distilled water and 95% ethanol until the filtrate was neutral, and then dried in an oven at 80°C for 24 h (Wang *et al*. 2010). The cellulose contents of corn stalk cellulose and rice straw cellulose were 98.7% and 98.3%, respectively and the ash contents were 2.7% and 8.3%, respectively (Wang and Cheng 2011). All other chemicals in this study were reagent grade. Microcrystalline cellulose of guaranteed reagent grade was purchased from Sinopharm Chemical Reagent Co. Ltd, China. The solvents used were distilled water and analytical reagent grade ethanol and acetone.

## Apparatus and Experimental Procedure

The liquefaction experiments were carried out using a floor stand 1.0 L autoclave (PARR 4521M, USA). It is rated up to a working pressure of 13 MPa and a working temperature of 350°C. A PID controller was used to control the temperature of the reactor. In a typical liquefaction experiment, the reactor was loaded with 8 g cellulose and 120 mL ethanol. Then the reactor was purged 3 times with nitrogen to remove the air/oxygen in the reactor airspace. Agitation was set at 250 rpm and maintained for all experiments. The reactor was heated up, and the temperature was maintained at the set temperature for the desired holding time. After the reaction was completed, the reactor was cooled down rapidly to room temperature by means of cooling coils, which were installed inside the reactor. A serpentine coil tubing 0.5 inch offers a large and effective cooling area with cooling water at room temperature. Once the reactor was cooled to room temperature, the density of gas was estimated using a gas bag by measuring the bulk and quality of the gaseous component. The bulk of gas was estimated by expelling water from the measuring cylinder. The gas products were not analyzed in this work since our main interest is in the liquid products. When the autoclave was opened, the reaction mixture was removed for separation. The procedure for the separation is shown in Fig. 1.

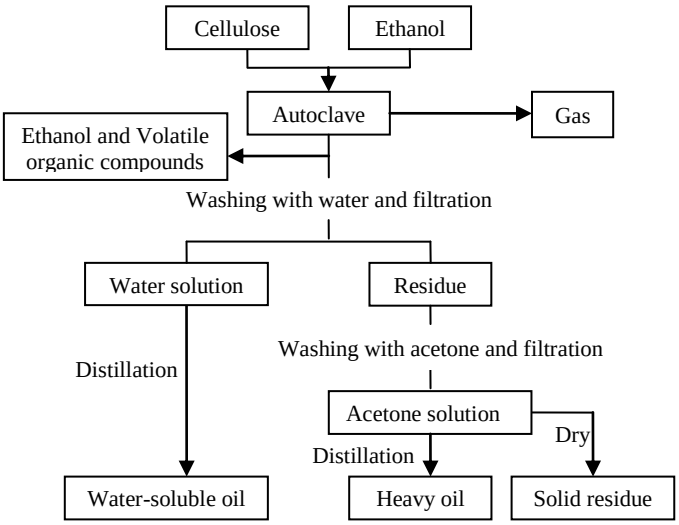


**Fig. 1.** Procedure for separation of products

In order to study the effect of reaction conditions on the cellulose liquefaction, the reaction system was divided into a gas fraction (GA), a water-soluble oil fraction (WSO), a heavy oil fraction (HO), a volatile organic compounds fraction (VO), and a solid residue fraction (SR) based on the characteristics of the materials and liquefaction products. The entire yield of each fraction was calculated on a dry basis. Two to three duplicate runs were conducted for all of the experimental conditions, and the error between the runs under the same conditions was ensured within 8%.

The results obtained in this study were reported using the parameters defined as,

$$Y_{GA} = \frac{V_{GA} \times \rho_{GA}}{W_{Dry}} \times 100\% \quad (1)$$

$$Y_{WSO} = \frac{W_{WSO}}{W_{Dry}} \times 100\% \quad (2)$$

$$Y_{HO} = \frac{W_{HO}}{W_{Dry}} \times 100\% \quad (3)$$

$$Y_{SR} = \frac{W_{SR}}{W_{Dry}} \times 100\% \quad (4)$$

$$Y_{VO} = 100\text{wt}\% - Y_{GA} - Y_{WSO} - Y_{HO} - Y_{SR} \quad (5)$$

where YGA is the gas yield (wt %), YWSO is the water-soluble oil yield (wt %), YHO is the heavy oil yield (wt %), YVO is the volatile organic compounds yield (wt %), YSR is the residue yield (wt %), WDry is the mass of cellulose flour (g), WWSO is the mass of water-soluble oil (g), WHO is the mass of heavy oil (g), WSR is the mass of residue (g), VGA is the volume of gas (mL), and ρGA is the density of gas (g/mL).

## Experimental Analyses

Fourier transform infrared spectrometer (FT-IR) experiments were operated on a Nicolet iN10 FT-IR spectrophotometer (USA). The instrument was performed with a MCT detector, and the spectra were recorded in the region of 4000 to 650 $cm^{-1}$ at a resolution of 4 $cm^{-1}$.

The celluloses and residues were evaluated using an X-ray diffractometer to determine the degree of crystallinity. X-ray diffractometry in reflection mode was conducted using a Shimadzu XRD 6000 (Japan), with monochromic Cu Kα radiation (λ = 0.15145 nm) generated at 40 kV and 50 mA. The degree of crystallinity of the celluloses and residues were determined based on the formula by Segal *et al.* (1959) (Segal *et al.* 1959) as follows,

$$CrI = (1 - I_{002} / I_{am}) \times 100\% \quad (1)$$

in which $I_{002}$ is the intensity for the crystalline portion of biomass (*i.e.*, cellulose) at about $2\theta = 22.6°$, and $I_{am}$ is the peak for the amorphous portion (*i.e.*, cellulose, hemicelluloses, and lignin) at about $2\theta = 18.7°$ in most literature. Each XRD experiment was repeated twice, and the relative errors were within 1.5%.

Chemical compositions of the water-soluble oil, heavy oil, and volatile organic compounds were identified using a HP5890GC/5971 mass spectrometer with a Restek Rxi-5 Sil Ms column (30 m, 0.25 mm i.d.). The oven temperature was programmed at 45°C for 1.5 min and then increased to 320°C at 20°C/min, and finally held with an

isothermal for 5 to 75 min. The injector temperature was 250°C and the spiltless injection size was 1 μL. The flow rate of the carrier gas (Helium) was 1.0 mL/min. The ion source temperature was 280°C for the mass selective detector. The compounds were identified by a comparison with the NIST Mass Spectral Database.

## RESULTS AND DISCUSSION

### Effect of Reaction Temperature on Distribution of Yields of Celluloses

Liquefaction experiments investigated the reaction mechanism of cellulose liquefaction in sub- and super-critical ethanol. The experiments were performed in pure ethanol at temperatures from 200 to 330°C under the pressure from 2 to 8 MPa. When temperature was 305°C, the reaction pressure was 6.4 MPa, and the highest level was higher than the critical point of ethanol (243°C, 6.4 MPa), which was in super-critical ethanol.

One of the most important parameters accelerating the reaction rate in the liquefaction process is the temperature. The fraction yields from the liquefaction of the three samples in ethanol at various temperatures ranging from 200°C to 330°C for 30 min are shown in Fig. 2; low SR yields were obtained at high temperatures for all liquefaction experiments (Fig. 2F). Regardless of all the samples and liquefaction experiments, the GA yield showed an identical trend with increasing reaction temperature, and the GA yield of celluloses increased by 27.6% (corn stalk cellulose), 17.1% (rice straw cellulose), and 14.8% (microcrystalline cellulose) from 200°C to 330°C (Fig. 2A). The liquid products which were the targeted products in biomass liquefaction were composed of WSO and HO. WSO mainly consisted of simple organic acids, alcohols, furfural, sugars, *etc*., which were primarily formed from the conversion of cellulose and hemicelluloses via de-polymerization and hydrolysis reactions (Behrendt *et al.* 2008; Xu and Lancaster 2008). In contrast, the HO, primarily composed of phenols, phenolic compounds, as well as long-chain carboxylic acids, esters, *etc*., results from the degradation/pyrolysis of lignin and from the dehydration of intermediate products derived from holocelluloses (Behrendt *et al.* 2008; Xu and Lancaster 2008). For all the samples liquefaction, the yield of WSO increased with an increase in temperature at first, and then decreased with an increase in temperature. The WSO yield of rice straw cellulose was highest (17.2%) at 280°C. The HO yields increased continuously with increasing temperature over the whole range of temperatures tested, and HO yields of different celluloses increased continuously from 1.2% to 13.4% (corn stalk cellulose), 0.7% to 11.7% (rice straw cellulose), and 1.9% to 11.4% (microcrystalline cellulose). From these results, it was also concluded that the HO resulted from the dehydration of intermediate products, such as WSO, derived from cellulose. For the microcrystalline cellulose liquefaction experiment, the bio-oil yield increased from 2.8% to 19.9% as the final temperature rose from 200°C to 320°C (Fig. 2B and 2C). Then, the bio-oil yield decreased to 18.9% with the temperature increasing to 330°C. The maximum yield of 18.9% was reached at 320°C (Fig. 2E). Additionally, it has been widely accepted that low-molecular-weight carbohydrates, present in the WSO as a product of cellulose hydrolysis, would occur at a high temperature to form oily intermediates, which would further be condensed into SR (Osada *et al.* 2006). For cornstalk cellulose and rice straw cellulose in the liquefaction experiments, the VO yields increased first and then decreased with increasing reaction temperature (Fig. 2D). The possible reasons to account for the change of the VO yield at

a higher temperature are: (1) The secondary decompositions became active at higher temperatures which led to the formation of GA and VO fraction, and (2) The condensation, cyclization, and re-polymerization of VO fraction led to the HO and SR formation (Liu *et al.* 2012a; Xu *et al.* 2008).

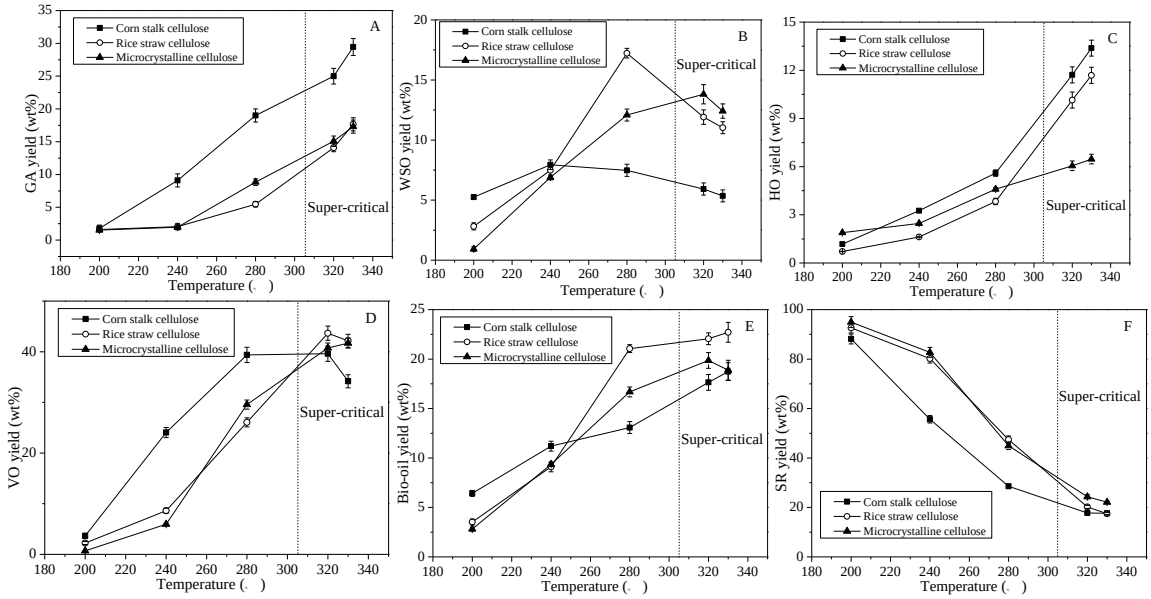


**Fig. 2.** Effect of temperature on distribution of yields of celluloses (Conditions: residence time of 30 min, 8 g of samples, and 120 mL of ethanol)

## Effect of Retention Time on Distribution of Yields of Celluloses

Figure 3 shows the effect of retention time on yields in the liquefaction of the three samples in super-critical ethanol (320°C, 6.89 MPa). When the reaction temperature reached 320°C, the GA yields from liquefaction of the three samples were 23.1% (cornstalk cellulose), 12.2% (rice straw cellulose), and 11.9% (microcrystalline cellulose). When the retention time increased to 120 min, the GA yields increased to 32.5% (cornstalk cellulose), 18.2% (rice straw cellulose), and 19.8% (microcrystalline cellulose), at the same temperature. Most researchers agree that bio-oil yield is higher with shorter retention times, as sustained reactions can decompose and/or convert the bio-oil to low molecular chemicals and solid residue (Yang *et al.* 2004). In our study, the yields of HO increased with an increase in retention time for all the samples subjected to liquefaction, while the WSO yields were lower at the shorter retention time. The HO yields were highest for 15.7%, 13.1%, and 9.1% at retention time 120 min, while WSO yields of celluloses reached the highest values of 7.1%, 17.0%, and 16.8% at retention time 0 min. Additionally, the total bio-oil (WSO + HO) yields appeared to level-off at around 30 min to 90 min, suggesting that a longer retention time was not necessary for a higher yield of the bio-oil product. Therefore, operating the reactor system at a shorter retention time was favorable because the rate of production would be higher and heat loss per unit mass of bio-oil produced could be significantly lower for a fixed reactor volume, making the process more energy efficient.

The effect of different samples on liquefaction in ethanol with various times can be clearly seen from the fraction yields. As can be seen from Fig. 3E, the VO yields showed different trends. These results could be explained by the different raw material characterization.

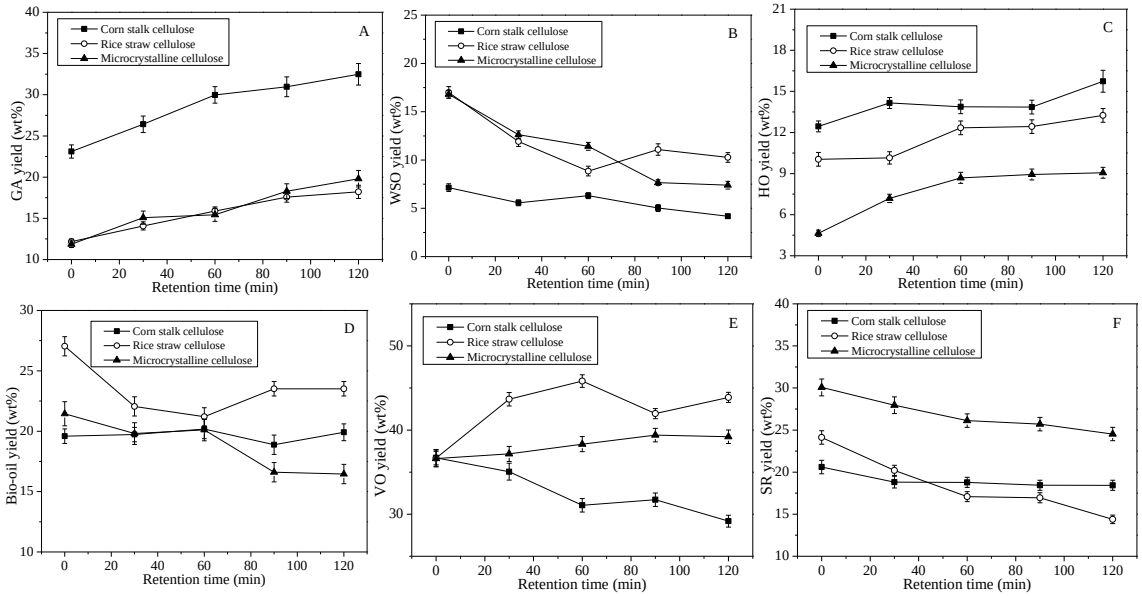


**Fig. 3.** Effect of retention time on distribution of yields of celluloses (Conditions: temperature of 320°C, 8 g of samples, and 120 mL of ethanol)

## Effect of Cellulose/Ethanol Ratio on Distribution of Yields of Celluloses

Experiments of the celluloses liquefied in solvent with different cellulose/ethanol (g/mL) ratios were carried out at 320°C, with 120 mL of ethanol and a retention time of 30 min. The results are presented in Fig. 4. When the ratio was higher than the ratio of 1/30, the yield of SR increased (Fig. 4F). The formation of SR was inhibited, and then the conversion was promoted by adding high ethanol amount. When the ratio was higher than the ratio of 1/30, the yield of SR increased. The major functions of solvents during the liquefaction process were to decompose the biomass and to provide active hydrogen. The presence of active hydrogen could stabilize liquefaction intermediates and prevent them from forming residue compounds.

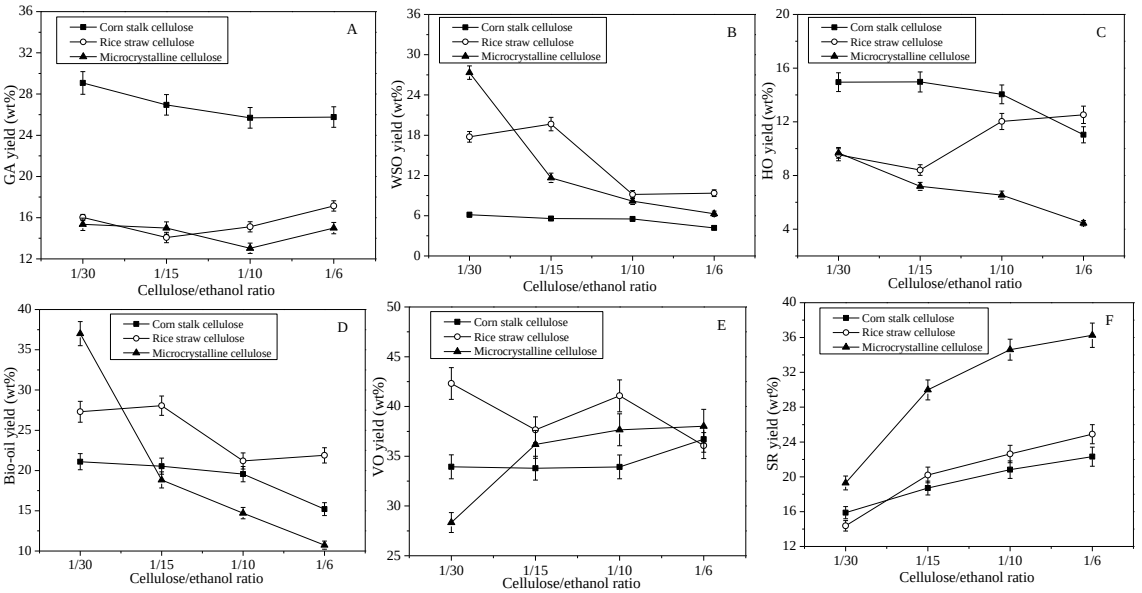


**Fig. 4.** Effect of cellulose/ethanol ratio on distribution of yields of celluloses (Conditions: temperature of 320°C, retention time of 30 min, 120 mL of ethanol)

In this study, the capability of ethanol as hydrogen-donor, which was promoted in the supercritical condition, might lead to stabilization of the free radicals generated from the liquefaction of celluloses. It could be clearly seen that the yields of bio-oil from the liquefaction of celluloses at the ratio of 1/30 was higher than that in other runs. It could be concluded that hydrolysis played an important role in the liquefaction of celluloses. As shown in Fig. 4A, the GA yields decreased with a decrease in cellulose/ethanol ratios first, and then increased as the ethanol was further added to the system. The effect of different samples on the liquefaction process at different cellulose/ethanol ratios could be clearly seen from the VO yields. These results might be due to the same reason with the mechanism in Section Effect of Retention Time on Distribution of Yields of Celluloses, which was caused by the different raw material characterization and the mechanism of the two reactions (hydrolysis and re-polymerization) involved in the liquefaction process.

## FT-IR Analysis

In order to reveal the liquefaction process of the three celluloses, FT-IR analyses of the SRs during celluloses liquefaction in sup- and super-critical ethanol were carried out. FT-IR spectra of the raw celluloses and SRs obtained at the five reaction temperatures of 200, 240, 280, 320, and 330°C for 30 min during the heating process are shown in Fig. 5. According to the literature (Liu 2006; Sun *et al.* 2004; Colom and Carrillo 2002), the bands in the spectra of celluloses before liquefaction in ethanol and SR were assigned as follows: The bands at 3362 $cm^{-1}$ are caused by the stretching of H-bonded OH groups, and that at 2900 $cm^{-1}$ relates to the C-H stretching. The band at 1615 $cm^{-1}$ is attributed to the bending mode of the absorbed water. A small peak at 1460 $cm^{-1}$ relates to the $CH_2$ symmetric bending. The absorbances at 1375 and 1320 $cm^{-1}$ originate from the O-H and C-H bending and C-C and C-O stretching. The peak at 1160 $cm^{-1}$ arises from C-O anti-symmetric bridge stretching. The C-O-C pyranose ring skeletal vibration gives a prominent band at 1045 $cm^{-1}$. A small sharp peak at 910 $cm^{-1}$ corresponds to the glycosidic $C_1$-H deformation with ring vibration contribution and OH bending, which is characteristic of β-glycosidic linkages between glucose in cellulose. In summary, the absorptions at 3362, 2900, 1615, 1460, 1374, 1320, 1160, 1045, and 910 $cm^{-1}$ are associated with the typical values of cellulose.

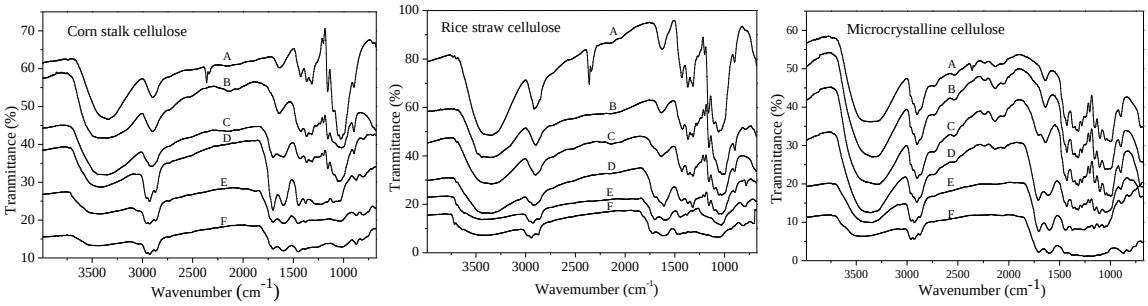


**Fig. 5.** FT-IR spectra of celluloses before and after liquefaction in sub- and super-critical ethanol, (A-raw cellulose, B-200°C, C-240°C, D-280°C, E-320°C, F-330°C)

The band at 1320 $cm^{-1}$ almost disappeared after 200°C liquefaction. This indicates that the chemical bond of C-C and C-O stretching in cellulose decomposition preceded other bonds in all the samples liquefaction experiments. As shown in Fig. 5, the band at 1160 $cm^{-1}$ almost disappeared at the temperatures of 280°C, 320°C, and 330°C for cornstalk cellulose, rice straw cellulose, and microcrystalline cellulose liquefaction,

respectively. The character of cellulose (such as crystalline structure) may be largely responsible for the decomposition of cellulose in sub- and super-critical ethanol. It is worth noting that a new band at 1705 $cm^{-1}$ was found in SR spectra at the higher temperatures as compared to raw celluloses, indicating that the structure of celluloses changed after liquefaction.

## GC-MS Analysis

The identification of major components of the VO, WSO, and HO products from liquefaction of the three samples was achieved through GC-MS analysis. Due to the complex composition of the products, the perfect separation of all the peaks was not possible. Only those separated products that arose in considerable amounts were evaluated, based on the peak areas of selected characteristic molecular or fragment ion chromatograms. Tables 1, 2, and 3 shows the comparison of the identified compounds in the products obtained from the liquefaction of the three samples at 320°C for 30 min.

During the studies conducted in recent years, the liquefaction products usually obtained from biomass (*i.e.*, cellulose, hemicelluloses, and lignin) liquefaction or pyrolysis have been analyzed by GC-MS. Xiu *et al.* (2010) studied the hydrothermal liquefaction of swine manure to bio-oil. They found that the bio-oil products were mainly composed of aromatic hydrocarbons, carbonyl group, alkenes, nitrogenous compounds, carboxylic acids, phenol, and their derivatives. As demonstrated in many previous studies, the WSO from biomass in a liquefaction process consists of carbohydrates, acetic acids, pyran derivatives, and aldehydes – mainly the decomposition products from the cellulose and hemicelluloses (Holgate *et al.* 1995; Jakab *et al.* 1997). In this study, the WSO comprises a very complex mixture of organic compounds of 6 to 12 carbons. Clearly, acids, esters, and furans were identified as the main compounds, such as 2-methyl-propanoic acid ethyl ester, 4-hydroxy-butanoic acid, butyl-2-butendioic acid, 2-furanmethyanol, and butyl-2-butendioic acid. The presence of acids in the bio-oil is undesirable because of the corrosive effects. As widely agreed by many researchers, the major components of HO primarily come from the decomposition of lignin, and they might also form from cellulose through hydrolysis to sugars, followed by dehydration and ring closure reactions (Zhang *et al.* 2010; Liu *et al.* 2011a,b). In fact, the HOs formed from the degradation of celluloses were a complex mixture of organic compounds of 6 to 20 carbons. As shown in Table 2, the HO products were identified to be mainly composed of 4-hydroxy-4-methyl-2-pentanone, 2-methyl-propanoic acid ethyl ester, butanedioic acid diethyl ester, ethylpentadecanoate, 5-ethoxymethyl furfural, *etc*. The components of the VO obtained from cypress liquefaction in hydrothermal liquefaction were observed in the paper. As reported, the VO product was mainly composed of a mixture of organic compounds of 5 to 7 carbons, such as furfural, 5-methyl-2-furancarboxaldehyde, and 2-methoxy-phenol, formed from the decomposition of hemicelluloses and lignin (Liu *et al.* 2012a). As shown in Table 3, the most important compounds present in VO obtained from celluloses liquefaction were 4-oxo-pentanoic acid ethyl ester, 2-methyl-cyclopentanone, 1-hydroxy-2-propanone, 2-hydroxy-propanoic acid ethyl ester, and so on. In addition, it can be seen that the compositional differences were relatively large among the VO, WSO, and HO originating from various samples. The differences of structure and components in bio-oils obtained from the celluloses liquefaction can be attributed to the different character of celluloses. Therefore, it can be concluded that the different celluloses had an important effect on the formation of various compounds in the liquefaction products.

**Table 1.** Identification of Compounds of Water-Soluble Oil in Supercritical Ethanol by GC-MS Analysis Obtained from Different Cellulose at 320°C for 30 Minutes

| No. | RT(min) | Compound | A | | B | | C | |
|---|---|---|---|---|---|---|---|---|
| | | | Content (%) | SI | Content (%) | SI | Content (%) | SI |
| 1 | 8.7 | 2-Methyl-2-cyclopentenone | 4.1 | 813 | | | | |
| 2 | 11.0 | 2-Furanmethanol, tetrahydro- | 2.4 | 858 | | | | |
| 3 | 11.5 | Propanoic acid, 2-methyl-, ethyl ester | 26.9 | 767 | | | | |
| 4 | 12.1 | 1,2-Propanediol | | | 7.7 | 859 | 1.9 | 915 |
| 5 | 12.9 | 1,2-Ethanediol | | | 3.9 | 894 | | |
| 6 | 13.3 | Butanoic acid, 4-hydroxy- | 4.3 | 863 | | | | |
| 7 | 13.6 | 2-Furanmethyanol | 8.9 | 849 | | | | |
| 8 | 16.1 | 2-Cyclopenten-1-one, 3-ethyl-2-hydroxy- | 3.7 | 814 | | | | |
| 9 | 16.8 | 2-Cyclopenten-1-one, 2-hydroxy-3-methyl- | 1.4 | 905 | 4.5 | 912 | 5.4 | 905 |
| 10 | 18.6 | Butyl-2-Butendioic acid | 10.8 | 824 | | | | |
| 11 | 21.2 | 5-Methyl-6-isopropyl-.delta.-valerolactone | | | | | 2.9 | 858 |
| 12 | 21.5 | Hexanoic acid, 2-ethyl-, ethyl ester | | | | | 2.8 | 801 |
| 13 | 24.8 | 4-Heptanol, 2,6-dimethyl- | | | 5.7 | 808 | | |
| 14 | 26.3 | Di-et mesuccinate | | | | | 3.9 | 796 |
| 15 | 27.3 | Guanosine | | | 6. 3 | 818 | 6.9 | 840 |
| 16 | 29.0 | 2-Furancarboxaldehyde, 5-(hydroxymethyl)- | | | | | 3.7 | 841 |
| 17 | 29.3 | 1,3,5-Triazine-2,4-diamine, 6-chloro-N-ethyl- | | | 2.8 | 791 | | |
| 18 | 29.4 | 3,3-Difluoro-1,2-dipropylcyclopropene | | | | | 7.3 | 813 |
| 19 | 31.2 | 1,2,4-Cyclopentanetriol | | | 6.3 | 798 | | |
| 20 | 34.1 | Hexanoic acid, 3-hydroxy-, ethyl ester | | | 3.7 | 815 | | |
| 21 | 35.1 | Hexadecanoic acid | | | 7.1 | 889 | 2.8 | 882 |
| 22 | 38.8 | 9-Octadecenoic acid(z)- | | | 5.8 | 873 | 2.4 | 861 |

"A, B, and C" indicate cornstalk cellulose, rice straw cellulose, and microcrystalline cellulose, respectively.

## X-ray Diffraction Analysis

Thermo-chemical processes can change the cellulose crystalline structure by disrupting inter/intra hydrogen bonding of cellulose chains (Mosier *et al.* 2005). X-ray measurements of the crystallinity index (CrI) are the best option to estimate thermo-chemical impacts on biomass crystallinity. To examine the evolution of the crystalline forms in the cellulose samples before and after liquefaction in sub- and super-critical ethanol, X-ray diffraction (XRD) measurements were carried out.

**Table 2.** Identification of Compounds of Heavy-oil in Supercritical Ethanol by GC-MS Analysis Obtained from Different Cellulose at 320°C for 30 Minutes

| NO. | RT(min) | Compound | A | | B | | C | |
|---|---|---|---|---|---|---|---|---|
| | | | Content (%) | SI | Content (%) | SI | Content (%) | SI |
| 1 | 8.5 | 2-Pentanone, 4-Hydroxy-4-Methyl- | 26.6 | 891 | 27.1 | 898 | 9.1 | 881 |
| 2 | 11.5 | Propanoic acid, 2-Methyl-, Ethyl ester | 19.4 | 808 | | | | |
| 3 | 12.6 | Pentanoic acid, 4-oxo-, ethyl ester | | | | | 4.8 | 893 |
| 4 | 13.1 | Di-et mesuccinate | | | | | 3.9 | 823 |
| 5 | 13.8 | Butanedioic acid, diethyl ester | 2.0 | 840 | | | 3.5 | 851 |
| 6 | 15.8 | Pentanedioic acid, diethyl ester | 4.6 | 913 | | | 2.8 | 831 |
| 7 | 16.7 | 2-Cyclopenten-1-one,2-hydroxy-3-methyl- | | | | | 5.1 | 875 |
| 8 | 18.8 | 5-Ethoxymethyl furfural | | | | | 8.6 | 802 |
| 9 | 23.2 | Phenol, 2-methoxy-4-(2-propenyl)- | | | 13.4 | 926 | 11.9 | 932 |
| 10 | 24.6 | Hexadecanoic acid, ethyl ester | | | 14.1 | 921 | 1.5 | 850 |
| 11 | 28.1 | Octadecanoic acid, ethyl ester | | | 5.5 | 843 | | |
| 12 | 28.2 | Ethylpentadecanoate | 3.4 | 808 | | | | |
| 13 | 34.1 | Pentadecanoic acid | | | | | 15.2 | 861 |
| 14 | 34.4 | 9,10-Dideutero octadecanoic acid | | | | | 2.6 | 795 |
| 15 | 35.1 | Hexadecanoic acid | | | 11.5 | 893 | | |
| 16 | 37.4 | Octadecanoic acid, ethyl ester | | | 5.4 | 848 | | |
| 17 | 38.9 | Ethyl iso-allocholate | | | 6.9 | 828 | | |

"A, B, and C" indicate cornstalk cellulose, rice straw cellulose, and microcrystalline cellulose, respectively.

**Table 3.** Identification of Compounds of Volatile Organic Compounds in Super-critical Ethanol by GC-MS from Different Celluloses at 320°C for 30 Minutes

| No. | RT(min) | Compound | A | | B | | C | |
|---|---|---|---|---|---|---|---|---|
| | | | Content (%) | SI | Content (%) | SI | Content (%) | SI |
| 1 | 6.2 | Cyclopentanone, 2-methyl- | | | 0.98 | 911 | 0.61 | 881 |
| 2 | 7.7 | 2-Propanone, 1-hydroxy- | 3.7 | 804 | | | 9.6 | 854 |
| 3 | 8.2 | Propanoic acid, 2-hydroxy-, ethyl ester | | | | | 9.5 | 877 |
| 4 | 8.7 | 2-Cyclopenten-1-one, 2-methyl- | 4.1 | 934 | 1.8 | 903 | | |
| 5 | 9.1 | Butanoic acid, 2-hydroxy- ethyl ester | 6.9 | 854 | 6.9 | 852 | | |
| 6 | 9.3 | Acetic acid, hydroxyl-, ethyl ester | 4.7 | 851 | 7.4 | 817 | | |
| 7 | 9.8 | Acetic acid | | | | | 6.1 | 876 |
| 8 | 10.1 | 2-Furancarboxaldehyde | | | | | 10.9 | 930 |
| 9 | 10.8 | Mehanone, 1-(2-furanyl)- | | | | | 2.2 | 810 |
| 10 | 11.2 | 2-Butanone, 1-(acetyloxy)- | | | | | 2.9 | 871 |
| 11 | 11.5 | Propanoic acid, 2-methyl-, ethyl ester | 15.1 | 783 | 12.1 | 813 | | |
| 12 | 12.1 | 2-Furancarboxaldehyde, 5-methyl- | | | | | 8.5 | 925 |
| 13 | 12. 2 | 1,2-Propanediol | 4.1 | 890 | 2.8 | 887 | | |
| 14 | 12.6 | Pentanoic acid, 4-oxo-, ethyl ester | 1.8 | 893 | 2.1 | 896 | 3.2 | 885 |
| 15 | 13.1 | 2(3H)-Furanone, dihydro- | 2.9 | 923 | 2.5 | 889 | | |
| 16 | 13.8 | Butanedioic acid, diethyl ester | 1.2 | 905 | 1.3 | 911 | | |
| 17 | 16.8 | 2-Cyclopenten-1-one,2-hydroxy-3-methyl- | | | 2.4 | 916 | 3.1 | 899 |
| 18 | 27.9 | 9-Octadecenioc acid, methyl ester | 6.1 | 942 | 2.2 | 924 | | |

"A, B, and C" indicate cellulose from cornstalk, rice straw, and microcrystalline, respectively.

Figure 6 illustrates the XRD spectra of the celluloses and SR from liquefaction at various temperatures (200, 240, 280, 320, and 330°C). The X-ray diffraction pattern of the raw celluloses showed two peaks at $2\theta$ = 18.5° and 22.2°, typical of cellulose I. It has been well documented that these peaks correspond to the (110) and (200) planes of cellulose (Borysiak and Doczekalska 2005; Xu and Lad 2008). The two peaks derived from cellulose I almost weakened at the temperature of 280°C for all the samples liquefaction. It is worth noting that two new XRD signals at $2\theta$ = 25.4° and 26.8° were detected at the higher temperatures (such as 320°C and 330°C), as shown in Fig. 6. These new peaks might be attributed to the diffraction lines of plane (200) of amorphous carbon and turbostratic carbon (Tsubouchi *et al.* 2003). The crystallinity index (CrI) for all samples was calculated from the XRD data, and the results are summarized in Table 4. According to the results of Table 4, the calculated CrI increased as temperature increased, and then it decreased for all the celluloses liquefaction tests, which indicated that the liquefaction reaction primarily occurred on amorphous zones of the celluloses at the low temperatures. The calculated CrI firstly increased from 59% to 67.3% (cornstalk cellulose), 57.4% to 67.0% (rice straw cellulose) at 200°C, and then decreased to 37% (cornstalk cellulose), 63.3% (rice straw cellulose) at 280°C, while the CrI of microcrystalline cellulose still decreased over the temperature tested, and the peak of crystalline zones for all the samples disappeared when temperature over 320°C. These observations, *i.e.*, weakened signals of celluloses in the resulting SRs at higher temperature, suggest conversion of the cellulose matrix into liquid/gas/carbon products (as evidenced previously in Figs. 2 to 4) and enhanced graphitization reactions of carbon at high temperatures.

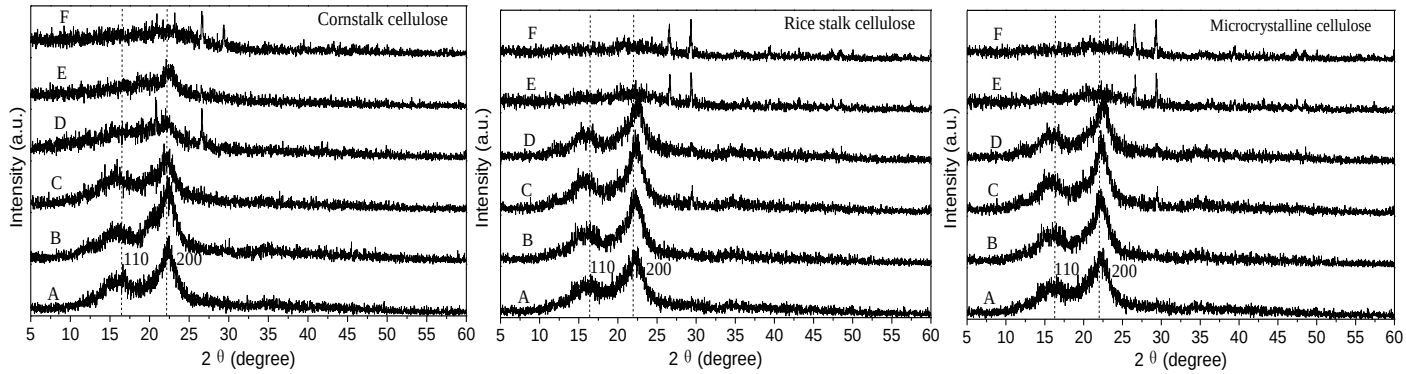


**Fig. 6.** X-ray diffraction patterns of celluloses before and after liquefaction in ethanol, (A-raw cellulose, B-200°C, C-240°C, D-280°C, E-320°C, F-330°C)

**Table 4.** Crystallinity Index (CrI) Values as Measured by X-ray Method for Celluloses Before and After Liquefaction in Ethanol

| Raw Material | Untreated | Temperature (°C) | | | | |
|---|---|---|---|---|---|---|
| | | 200 | 240 | 280 | 320 | 330 |
| Cornstalk cellulose | 59 | 67.3 | 47.6 | 37 | - | - |
| Rice straw cellulose | 57.4 | 67 | 63.5 | 63.3 | - | - |
| Microcrystalline cellulose | 88.6 | 88.5 | 86.2 | 70.8 | - | - |

"-" indicates a complete decomposition of amorphous cellulose.

## CONCLUSIONS

The results demonstrated the effect of reaction conditions on the distribution of yields during liquefaction of celluloses in sub- and super-critical ethanol at temperatures in the range 200 to 330°C. The following conclusions were reached:

1. For all the samples liquefaction, the yield of WSO increased with an increase in temperature at first, and then decreased with an increase in temperature, while the HO yields increased continuously with increasing temperature from 200 to 330°C. The VO yields increased first, and then decreased when the reaction temperature was increased for the cornstalk cellulose and rice straw cellulose liquefaction experiment. The yields of SR and WSO generally decreased obviously with retention time before 60 min, while the yield of HO increased over all the retention time, suggesting the occurrence of polymerization and condensation of the WSO and VO.

2. For the three samples, the SR yield of microcrystalline cellulose always was highest compared with corn stalk cellulose and rice straw cellulose at the same temperature, while the HO yield of microcrystalline cellulose always was lowest in the liquefaction process. At the same retention time in super-critical ethanol, the SR yield of microcrystalline cellulose was highest, suggesting that the microcrystalline cellulose was difficult liquefied.

3. FT-IR analysis of the SRs showed that the structure of celluloses changed after liquefaction. The GC-MS analysis showed that the VO, WSO, and HO comprised a mixture of organic compounds, which mainly included furfural, acids, furans, esters, and their derivatives. XRD analysis revealed that the decomposition reaction primarily occurred within amorphous zones of the celluloses at the low temperatures, and when the temperature was over 320°C, the conversion of cellulose matrix into liquid/gas/carbon products occurred and graphitization reactions of carbon were enhanced.

## ACKNOWLEDGEMENTS

We sincerely acknowledge the financial support by Guangdong Provincial Science and Technology program Foundation of China (2009B050700037), and the National Natural Science Foundation of China (21176097).

## REFERENCES CITED

Behrendt, F., Neubauer, Y., Oevermann, M., Wilmes, B., and Zobel, N. (2008). "Direct liquefaction of biomass," *Chem. Eng. Technol.* 31(5), 667-677.

Borysiak, S., and Doczekalska, B. (2005). "X-ray diffraction study of pine wood treated with NaOH," *Fibres Text. East. Eur.* 13(5), 87-89.

Colom, X., and Carrillo, F. (2002). "Crystallinity changes in lyocell and viscose-type fibers by caustic treatment," *Eur. Polym. J.* 38(11), 2225-2230.

Demirbas, A. (2000). "Mechanisms of liquefaction and pyrolysis reactions of biomass," *Energy Convers. Manage.* 41(6), 633-646.

Gil, M. V., Casal, D., Pevida, C., Pis, J. J., and Rubiera, F. (2010). "Thermal behaviour and kinetics of coal/biomass blends during co-combustion," *Bioresour. Technol.* 101(14), 5601-5608.

Holgate, H. R., Meyer, J. C., and Tester, J. W. (1995). "Glucose hydrolysis and oxidation in supercritical water," *AIChE J.* 41(3), 637-647.

Jakab, E., Liu, K., and Meuzelaar, H. L. C. (1997). "Thermal decomposition of wood and cellulose in the presence of solvent vapors," *Ind. Eng. Chem. Res.* 36(6), 2087-2095.

Kruse, A., and Gawlik, A. (2003). "Biomass conversion in water at 330-410 °C and 30-50 MPa. Identification of key compounds for indicating different chemical reaction pathways," *Ind. Eng. Chem. Res.* 42(2), 267-279.

Lawther, J. M., Sun, R. C., and Banks, W. B. (1995). "Extraction, fractionation, and characterization of structural polysaccharides from wheat straw," *J. Agric. Food Chem.* 43(3), 667-675.

Liu, C. F., Ren, J. L., Xu, F., Liu, J. J., Sun, J. X., and Sun, R. C. (2006). "Isolation and characterization of cellulose obtained from ultrasonic irradiated sugarcane bagasse," *J. Agric. Food Chem.* 54(16), 5742-5748.

Liu, H. M., Feng, B., and Sun, R. C. (2011a). "Acid-chlorite pretreatment and liquefaction of cornstalk in hot-compressed water for bio-oil production," *J. Agric. Food Chem.* 59(19), 10524-10531.

Liu, H. M., Feng, B., and Sun, R. C. (2011b). "Enhanced bio-oil yield from liquefaction of cornstalk in sub- and supercritical ethanol by acid-chlorite pretreatment," *Ind. Eng. Chem. Res.* 50(19), 10928-10935.

Liu, H. M., Xie, X. A., Feng, B., and Sun, R. C. (2011c). "Effect of catalysts on 5-lump distribution of cornstalk liquefaction in sub-critical ethanol," *BioResources* 6(3), 2592-2604.

Liu, H. M., Xie, X. A., Li, M. F., and Sun, R. C. (2012a). "Hydrothermal liquefaction of cypress: Effect of reaction conditions on 5-lump distribution and composition," *J. Anal. App. Pyrol.* 94, 177-183.

Liu, H. M., Xie, X. A., Ren, J. L., and Sun, R. C. (2012b). "8-Lump reaction pathways of cornstalk liquefaction in sub- and super-critical ethanol," *Ind. Crop. Prod.* 35(1), 250-256.

Liu, Z. G., and Zhang, F. S. (2008). "Effects of various solvents on the liquefaction of biomass to produce fuels and chemical feedstocks," *Energy Convers. Manage.* 49(12), 3498-3504.

Mosier, N., Wyman, C., Dale, B., Elander, R., Lee, Y. Y., Holtzapple, M., and Ladisch, M. (2005). "Features of promising technologies for pretreatment of lignocellulosic biomass," *Bioresour. Technol.* 96(6), 673-686.

Munir, S., Daood, S. S., Nimmo, W., Cunliffe, A. M., and Gibbs, B. M. (2009). "Thermal analysis and devolatilization kinetics of cotton stalk, sugar cane bagasse and shea meal under nitrogen and air atmospheres," *Bioresour. Technol.* 100(3), 1413-1418.

Osada, M., Sato, T., Watanabe, M., Shirai, M., and Arai, K. (2006). "Catalytic gasification of wood biomass in subcritical and supercritical water," *Combust. Sci. Technol.* 178(1-3), 537-552.

Ozcimen, D., and Karaosmanoglu, F. (2004). "Production and characterization of bio-oil and biochar from rapeseed cake," *Renew. Energ.* 29(5), 779-787.

Segal, L., Creely, J. J., Martin Jr, A. E., and Conrad, C. M. (1959). "An empirical method for estimating the degree of crystallinity of native cellulose using the X-Ray diffractometer," *Text. Res. J.* 29(10), 786-794.

Simkovic, I., and Csomorova, K. (2006). "Thermogravimetric analysis of agricultural residues: Oxygen effect and environmental impact," *J. Appl. Polym. Sci.* 100(2), 1318-1322.

Sun, X. F., Sun, R. C., Su, Y. Q., and Sun, J. X. (2004). "Comparative study of crude and purified cellulose from wheat straw," *J. Agric. Food Chem.* 52(4), 839-847.

Tsubouchi, N., Xu, C. B., and Ohtsuka, Y. (2003). "Carbon crystallization during high-temperature pyrolysis of coals and the enhancement by calcium," *Energ. Fuel* 17(5), 1119-1125.

Van de Velden, M., Baeyens, J., Brems, A., Janssens, B., and Dewil, R. (2010). "Fundamentals, kinetics and endothermicity of the biomass pyrolysis reaction," *Renew. Energ.* 35(1), 232-242.

Wang, M. C., Xu, C. B., and Leitch, M. (2009). "Liquefaction of cornstalk in hot-compressed phenol-water medium to phenolic feedstock for the synthesis of phenol–formaldehyde resin," *Bioresour. Technol.* 100(7), 2305-2307.

Wang, L., Shen, S. Q., Yang, S. H., Shi, and X. G. (2010). Experimental investigation of pyrolysis process of corn straw," *Int. J. Low-Carbon Tech.* 5(4), 182-185.

Wang, L. F., and Cheng, Y. C. (2011). "Determination the content of cellulose by nitric acid-ethanol method," *Chemical Research* 22(4), 52-55.

Xiu, S. N., Shahbazi, A., Shirley, V., and Cheng, D. (2010). "Hydrothermal pyrolysis of swine manure to bio-oil: Effects of operating parameters on products yield and characterization of bio-oil," *J. Anal. Appl. Pyrol.* 88(1), 73-79.

Xu, C. B., and Lad, N. (2008). "Production of heavy oils with high caloric values by direct of liquefaction of woody biomass in sub/near-critical water," *Energ. Fuel* 22(1), 635-642.

Xu, C. B., and Lancaster, J. (2008). "Conversion of secondary pulp/paper sludge powder to liquid oil products for energy recovery by direct liquefaction in hot-compressed water," *Water Res.* 42(6-7), 1571-1582.

Yang, Y. F., Feng, C. P., Inamori, Y., and Maekawa, T. (2004). "Analysis of energy conversion characteristics in liquefaction of algae," *Resour. Conserv. Recy.* 43(1), 21-33.

Yanik, J., Kornmayer, C., Saglam, M., and Yuksel, M. (2007). "Fast pyrolysis of agricultural wastes: Characterization of pyrolysis products," *Fuel Process. Technol.* 88(10), 942-947.

Zhang, L. H., Xu, C. B., and Champagne, P. (2010). "Energy recovery from secondary pulp/paper-mill sludge and sewage sludge with supercritical water treatment," *Bioresour. Technol.* 101(8), 2713-2721.

Article submitted: March 19, 2012; Peer review completed: May 28, 2012; Revised version received: June 18, 2012; Second revised version: July 29, 2012; Accepted: December 3, 2012; Published: December 12, 2012.